The Importance of Magnetic Coupling through Atoms with Large Spin Densities—Structure and Magnetic Properties of *meso*-Tetrakis-(4′-*tert*-butylphenyl)porphinatomanganese(III) Hexacyanobutadienide, $[Mn^{III}TtBuPP]^{+}[C_4(CN)_6]^{\bullet -}$

Ken-ichi Sugiura, Atta M. Arif, Durrell K. Rittenberg, Jacques Schweizer, Lars Öhrstrom, Arthur J. Epstein, and Joel S. Miller*

Abstract: $[Mn^{III}TtBuPP]^{+}[C_4(CN)_6]^{\bullet -} \cdot 5PhMe$ [$Mn^{III}TtBuPP$ = *meso*-tetrakis-(4′-*tert*-butylphenyl)porphinatomanganese(III)] has been prepared and structurally and magnetically characterized. The uniform, linear-chain (1-D) coordination polymer comprises alternating cations and anions. The bond lengths in planar ion $[C_4(CN)_6]^{\bullet -}$ are 1.377(10) (CC–CC), 1.418(7) (C–CCC), 1.414 (C–CN), 1.457 (C–CNMn), 1.150 (C≡N), and 1.134 Å (C≡NMn). The Mn–N–C angle is 172.3(4)°, and the intrachain Mn···Mn separation is 10.685 Å. Each $[C_4(CN)_6]^{\bullet -}$ unit is bonded to two Mn^{III} atoms through the interior nitrogen atoms in a *trans*-μ_2-*N*-σ manner with N–Mn bond lengths of 2.353 Å. The $\tilde{\nu}_{CN}$ absorptions are at 2217 (w, br) and 2190 (m) cm^{-1}. Above 50 K the magnetic susceptibility of $[Mn^{III}TtBuPP]^{+}[C_4(CN)_6]^{\bullet -}$ can be fitted to the Curie–Weiss expression, $\chi \propto 1/(T-\theta)$, with an effective θ of −13 K. This is consistent with weak antiferromagnetic coupling, which is in contrast to the effective θ of +67 K for the uniform chain $[Mn^{III}OEP]^{+}[C_4(CN)_6]^{\bullet -}$ [OEP = octaethylporphinato]. Here, the $[C_4(CN)_6]^{\bullet -}$ units are bonded to the Mn^{III} centers through *endo* CN nitrogen atoms in a similar *trans*-μ_2 manner. Density functional theory MO calculations reveal that the spin density of the CN nitrogen atom bound to $[Mn^{III}TtBuPP]^{+}$ (0.019 $\mu_B Å^{-3}$) is significantly lower than that of the N atom bound to $[Mn^{III}OEP]^{+}$ (0.102 $\mu_B Å^{-3}$). This is consistent with the reduced spin coupling observed for $[Mn^{III}TtBuPP]^{+}[C_4(CN)_6]^{\bullet -}$ with respect to $[Mn^{III}OEP]^{+}[C_4(CN)_6]^{\bullet -}$, as evidenced by the lower θ value. The different orientations of the $[C_4(CN)_6]^{\bullet -}$ units—almost perpendicular (84.72°) for $[Mn^{III}TtBuPP]^{+}[C_4(CN)_6]^{\bullet -}$ and substantially tilted (32.1°) for $[Mn^{III}OEP]^{+}[C_4(CN)_6]^{\bullet -}$—may also contribute to the poorer overlap and weaker spin coupling. Hence, binding between sites with large spin densities is needed to stabilize strong ferromagnetic coupling.

Keywords
electron transfer · magnetic properties · metalloporphryins · polymers · spin density

Introduction

The study of strong magnetic materials consisting of molecular components is a growing area of contemporary interdisciplinary materials chemistry research.[1–4] Since the discovery of the bulk magnetic properties of $[MnTPP]^{+}[TCNE]^{\bullet -}$ (TPP = *meso*-tetraphenylporphinato, TCNE = tetracyanoethylene),[4] several new magnetic materials based on electron-transfer salts of metallomacrocycles have been reported.[5–10] As described for $[MnTPP]^{+}[TCNE]^{\bullet -}$, these magnets possess extended linear-chain (1-D) coordination polymer structures, which comprise alternating metallomacrocycle cations (D^{+}) and cyanocarbon radical anions ($A^{\bullet -}$) ($\cdots D^{+}A^{\bullet -}D^{+}A^{\bullet -}\cdots$). Strong effective ferromagnetic coupling is observed for the uniform chain $[Mn^{III}OEP]^{+}[C_4(CN)_6]^{\bullet -}$ (OEP = octaethylporphinato).[6] This is evidenced by the magnitude of the positive Weiss constant (θ = 67 K) obtained from a fit of the corrected molar magnetic susceptibility, χ, to the Curie–Weiss expression, $\chi \propto (T-\theta)^{-1}$. In contrast, the dimerized chain $[Mn^{III}OEP]^{+}[TCNE]^{\bullet -}$ has a low θ value (θ = 2.5 K). Hence, uniform chain structures of the type $\cdots D^{+}A^{\bullet -}D^{+}A^{\bullet -}\cdots$ are sought for achieving strong antiferromagnetic coupling.[6]

Owing to the relative ease of modifying the porphyrin structure, we decided to study the effect of introducing bulky *tert*-butyl groups at the 4′-position of the phenyl rings of the prototype [MnTPP][TCNE] magnet. This should enhance the one-dimensionality of the system by increasing the interchain separations. Since the exchange coupling J is inversely propor-

[*] Prof. J. S. Miller, Dr. K.-i. Sugiura, Dr. A. M. Arif, D. K. Rittenberg
Department of Chemistry, University of Utah
Salt Lake City, Utah 84112 (USA)
Fax: Int. code +(801)581-8433
e-mail: jsmiller@atlas.chem.utah.edu
Dr. J. Schweizer, L. Öhrstrom
DRFMC/SPCMS/MDN and DRFMC/SESAM
Centre d'Etudes Nucléaires, 38054 Grenoble (France)
Prof. A. J. Epstein
Department of Physics and Department of Physical Chemistry
Ohio State University, Columbus, Ohio 43210 (USA)

0947-6539/97/0301-0138 $ 15.00+.25/0

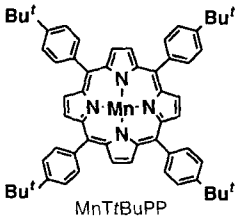

MnT*t*BuPP

tional to the separation r between spin sites (e.g., r^{-n}, $n \geq 6$ for superexchange pathways),[11] small increases in the interchain separation should have a dramatic effect on interchain J. This should lead to a reduction of the 3-D ordering temperature, T_c. The intrachain exchange coupling has the largest affect on θ. Assuming that the McConnell virtual charge transfer mechanism[12] is operative, θ is dependent on the separation of spin sites, the density of spin at each of the adjacent sites, and the angular relationship of the adjacent atom-centered orbitals. Herein we report the preparation and structure of *meso*-tetrakis(4′-*tert*-butylphenyl)porphinatomanganese(III) hexacyanobutadienide, $[Mn^{III}TtBuPP]^+[C_4(CN)_6]^{\bullet -}$, which possesses a uniform $\cdots D^+A^{\bullet -}D^+A^{\bullet -}\cdots$ chain, but unexpectedly has weak antiferromagnetic coupling.

Experimental Section

Synthesis: All manipulations were carried out under an atmosphere of nitrogen with standard Schlenck techniques or in a Vacuum Atmospheres glove box. Solvents used were predried and distilled from appropriate drying agents [13a]. $H_2TtBuPP$ was prepared by the general literature method [13b,c] from 4′-*tert*-butylbenzaldehyde (Aldrich). $[Mn^{III}TtBuPP][OAc]$ was prepared from $H_2TtBuPP$ and $Mn(OAc)_2$ [13d] and subsequently reduced to $Mn^{II}TtBuPP$ [13d] with $NaBH_4$ according to well-established methodologies (after we had started this project, $H_2TtBuPP$ was reported [13e]). Hexacyanobutadiene was prepared as described in the literature [14].

$[Mn^{III}TtBuPP]^+[C_4(CN)_6]^{\bullet -}$: $Mn^{II}TtBuPP$ (88.0 mg, 90.6 mmol) dissolved in toluene (30 mL) was added to $C_4(CN)_6$ (18.7 mg, 91.6 mmol) dissolved in toluene (110 mL) at room temperature. Crystals formed upon refrigeration of the sample at −40 °C were collected by filtration (yield: 42.3 mg, 0.28 mmol, 30%). IR (Nujol): $\tilde{\nu}_{CN}$ = 2217 (w, br), 2190 (m) cm^{-1}. Crystals immediately isolated for X-ray studies contained 5 equiv of toluene solvate, which were easily lost. The IR spectrum of the dried sample was identical to that of a fresh, solvated sample. Elemental analysis for $C_{70}H_{60}MnN_{10}$ (unsolvated sample), calcd (found): C 76.70 (76.57), H 5.52 (5.47), N 12.78 (12.70).

X-ray Structure Determination [20]: Crystals of the pentatoluene solvate suitable for single-crystal X-ray diffraction were obtained by refrigerating a dilute toluene solution. Cell constants and an orientation matrix for data collection were obtained by standard methods from 25 reflections at −80 °C. Systematic absences and subsequent least-squares refinement were used to determine the space group. During data collection the intensities of several representative reflections were measured as a check on crystal stability. There was no loss of intensity during data collection. Equivalent reflections were merged, and only those for which $I_o > 2\sigma(I)$ were included in the refinement, where $\sigma(F_o)^2$ is the standard deviation based on counting statistics. SHELEX-93 was used for the refinement. Data were also corrected for Lorentz and polarization factors. An empirical absorption correction of 1.99 cm^{-1} was applied. Crystallographic details are summarized in Table 1. The hydrogen atoms were isotopically refined using the riding model, by which the H atoms coordinates are reidealized before each refinement cycle and "ride" on the atoms to which they are attached. The toluenes occupy five different sites. Each is at half occupancy in the asymmetric unit and shows two orientation disorders. The FLAT instructions in SHELXL-93 was used to apply geometrical restraints. Owing to the high degree of disorder, only one toluene solvent was refined isotropically; the rest were refined anisotropically. The comparatively large $R1$ and residual peak values are due to disordered solvent and a methyl group.

Physical and Computation Methods: The 2–300 K magnetic susceptibility was determined on Quantum Design MPMS-21 T SQUID and Quantum Design PPMS-9AC9T AC/DC magnetometers. The diamagnetic correction of -900×10^{-6} emu mol^{-1} was used for $[Mn^{III}OEP]^+[C_4(CN)_6]^{\bullet -}$. DGAUSS was used for the density functional theory (DFT) calculations with a double-ζ split-valence and polarization basis set and a local approximation (DZVP-LSD) [15,16a]. The $[C_4(CN)_6]^{\bullet -}$ geometry used for the computations was that reported for $[Mn^{III}OEP]^+[C_4(CN)_6]^{\bullet -}$ [6].

Table 1. Crystallographic details for $[Mn^{III}TtBuPP]^+[C_4(CN)_6]^{\bullet -} \cdot 5\,PhMe$.

formula	$C_{105}H_{100}N_{10}Mn$
M_r	1556.89
space group	$P2_1/n$ (no. 15)
a, Å	16.137(4)
b, Å	10.685(3)
c, Å	26.221(7)
β, deg	92.29(2)
V, Å3	4518(2)
Z	2
ρ_{calcd}, g cm^{-3}	1.145
crystal dimensions, mm	0.44 × 0.42 × 0.38
radiation	$Mo_{K\alpha}$
absorption coefficient, cm^{-1}	1.99
T, °C	−80
scan mode	$\theta/2\theta$
2θ max, deg	23.99
$F(000)$	1650
total data measured	7343
unique data with $F_o^2 > 2\sigma F_o^2$	7061
final no. of variables	470
weighting scheme	$[\sigma^2(F_o)^2 + [0.1355P]^2 + 7.28P]^{-1}$
$R1$ [a]	0.084
$wR2$ [b]	0.021
largest residual, e $Å^{-3}$	0.75 (Mn and N3)

[a] $\frac{\sum||F_o| - |F_c||}{\sum|F_o|}$. [b] $\left[\frac{\sum w(F_o^2 - F_c^2)^2}{\sum wF_o^4}\right]^{1/2}$.

Results and Discussion

The structure determination reveals one half of an ordered $[Mn^{III}TtBuPP]^+[C_4(CN)_6]^{\bullet -}$ unit, where the cation and anion each reside on a center of symmetry (Figure 1). Also present are five molecules of toluene, which are disordered. The average Mn^{III}–N(ring) bond length is 2.006 Å, and the remaining intracation distances and angles are typical for Mn^{III} porphyrins. The planar hexacyanobutadienide CC bond lengths are 1.377(10) (CC=CC) and 1.418(7) Å (C–CCC), consistent with the radical anion.[14b] The C–CN distances average 1.414 Å, while the C–CNMn bond length is 1.457 Å. The C≡N and C≡NMn distances average 1.150 and 1.134 Å, respectively. These are similar to those observed for the $[MnOEP]^+$ salt (Table 2).[6]

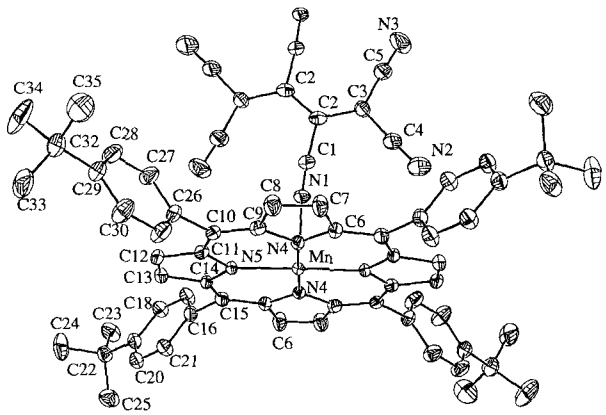

Fig. 1. ORTEP diagram of $[Mn^{III}TtBuPP]^+[C_4(CN)_6]^{\bullet -}$.

Table 2. Selected bond lengths for $[Mn^{III}TtBuPP]^+[C_4(CN)_6]^{\bullet -}$ and $[Mn^{III}OEP]^+[C_4(CN)_6]^{\bullet -}$.

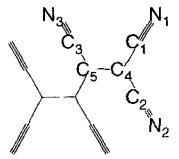

	[MnOEP]$^+$	[MnT*t*BuPP]$^+$		[MnOEP]$^+$	[MnT*t*BuPP]$^+$
C5–C5	1.366(12)	1.377(10)	C2–C4	1.410(10)	1.413(7)
C4–C5	1.432(11)	1.418(7)	C1–N1	1.140(9)	1.157(7)
C3–C5	1.446(11)	1.457(7)	C2–N2	1.138(9) [Mn]	1.142(9)
C1–C4	1.437(10)	1.415(8)	C3–N3	1.132(8)	1.134(6) [Mn]

The solid-state motif comprises 1-D $\cdots D^+A^{\bullet -}D^+A^{\bullet -}\cdots$ chains [D = MnT*t*BuPP; A = $C_4(CN)_6$], in which the $[C_4(CN)_6]^{\bullet -}$ units are *trans*-μ_2-interior-*N*-σ-bound to Mn with a N–Mn bond length of 2.353(4) Å (Figure 2). The Mn–N–C angle is 172.3(4)°, and the dihedral angle between the mean planes of $[MnTtBuPP]^+$ and $[C_4(CN)_6]^{\bullet -}$ is 84.72(14)°. The Mn–N–C angle is substantially larger than that reported for the $[MnOEP]^+$[6] and $[MnTPP]^+$[4, 5] salts (124.0(6) and 148.1(4)°, respectively). The 10.685 Å intrachain Mn$\cdots$Mn separation is 0.16 Å shorter than that observed for the $[MnOEP]^+$ salt.[6] The important intra- and interchain Mn$\cdots$Mn separations for $[MnTtBuPP][C_4(CN)_6]\cdot 5PhMe$ and $[MnOEP][C_4(CN)_6]$ are listed in Table 3. The key differences between the $[C_4(CN)_6]^{\bullet -}$ structures are 1) the mode of bonding—through the interior N atoms for $[MnTtBuPP]^+$ as opposed to the *endo* N atoms for $[MnOEP]^+$—and 2) the almost perpendicular (84.72°) orientation for $[MnTtBuPP]^+$ in contrast to the tilted one for $[MnOEP]^+$ (32.1°).

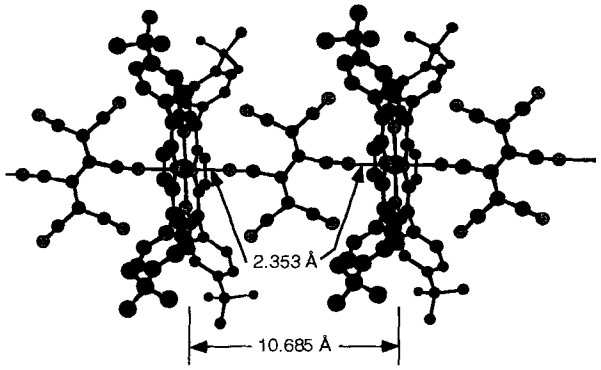

Fig. 2. Segment of a 1-D $\cdots D^+A^{\bullet -}D^+A^{\bullet -}\cdots$ chain showing interior-*trans*-μ2-*N*-σ-bonding of $[C_4(CN)_6]^{\bullet -}$ to $[Mn^{III}TtBuPP]^+$. For clarity, the toluene molecules of solvation are not shown.

The $\tilde{\nu}_{CN}$ absorptions at 2217 (w, br) and 2190 (m) cm^{-1} (Nujol) are in the range characteristic for $[C_4(CN)_6]^{\bullet -}$;[14b, c] however, they differ from isolated unbound $[C_4(CN)_6]^{\bullet -}$ (2185 (s) and 2168 (m) cm^{-1})[14b] and *endo-trans*-μ_2-Mn-bound $[C_4(CN)_6]^{\bullet -}$ (2193 (s) and 2150 (s) cm^{-1}).[6] They are characteristic for interior-*N*-*trans*-μ_2-Mn-bound $[C_4(CN)_6]^{\bullet -}$. Since the unit cell contains five equivalents of toluene, which are easily lost, the IR spectrum of the solvated solid was determined. The $\tilde{\nu}_{CN}$ absorptions are identical to that of samples that have lost substantial amounts of solvent; the gross structure is preserved.

The reciprocal of the corrected magnetic susceptibility (χ^{-1}) and the magnetic moment (μ) of $[MnTtBuPP][C_4(CN)_6]$ between 2–300 K are shown in Figure 3. Above ca. 50 K the susceptibility can be fitted to the Curie–Weiss expression, $\chi \propto 1/(T-\theta)$, with an effective θ of −13 K. This is in contrast to the θ values of 61 and 67 K reported for the uniformly chained $[MnTPP][TCNE]$[4, 5] and $[MnOEP][C_4(CN)_6]$,[6] respectively. Furthermore, it is less than the θ values reported for nonuniformly chained $[MnOEP][TCNE]$[6] and β-[MnPc][TCNE][10] (2.5 and 12 K, respectively; Pc = phthalocyanine). The observed room-temperature effective moment [$\mu_{eff} \equiv (8\chi T)^{1/2}$] of 4.91 μ_B is typical for this class of material.[4–6, 9, 10] No clear evidence of long-range magnetic ordering is observed.

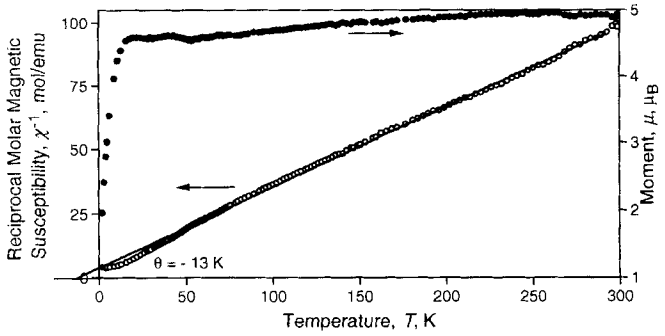

Fig. 3. Reciprocal molar magnetic susceptibility (χ^{-1}) and magnetic moment (μ) as a function of temperature for polycrystalline $[Mn^{III}TtBuPP]^+[C_4(CN)_6]^{\bullet -}$.

Table 3. Comparison of the intrachain and shortest interchain Mn$\cdots$Mn and Mn$\cdots$N distances [Å], and Mn–N–C angles [deg] for $[Mn^{III}TtBuPP]^+[C_4(CN)_6]^{\bullet -}$ and $[MnOEP]^+[C_4(CN)_6]^{\bullet -}$ [6].

Cation	Mn$\cdots$Mn intrachain [a]	Mn$\cdots$Mn interchain	Mn$\cdots$N intrachain	Mn$\cdots$N interchain	Interchain separations	∢Mn-N-C	∢MnOEP–$C_4(CN)_6$
$[MnOEP]^+$	10.844	8.023	2.419 [b]	7.507	7.903	124	32.1
		12.332		10.733	11.319		
		12.550		11.236	13.805		
		14.385					
$[MnTtBuPP]^+$	10.685	16.137	2.353 [b]	12.921	15.105	172.3	84.72
		16.034		13.487	15.669		
		16.465		15.280	16.137		
		16.552 [b]		15.563			

[a] *b* axis. [b] Two equivalent distances.

0947-6539/97/0301-0140 $ 15.00+.25/0 Chem. Eur. J. 1997, 3, No. 1

Similar to many ferromagnetically coupled molecule-based materials that contain $[TCNE]^{\bullet -}$,[2, 3] $[C_4(CN)_6]^{\bullet -}$ can also form materials with effective ferromagnetic coupling. $[Mn^{III}OEP]^+[C_4(CN)_6]^{\bullet -}$ has a uniform chain repeat distance of 10.844 Å and exhibits a large positive θ value of 67 K. Hence, the negative θ value for $[Mn^{III}TtBuPP]^+[C_4(CN)_6]^{\bullet -}$ is unexpected as it is inconsistent with the presence of the uniform $\cdots D^+A^{\bullet -}D^+A^{\bullet -}\cdots$ chain. In the $[Mn^{III}OEP]^+$ salt, the $[C_4(CN)_6]^{\bullet -}$ is bonded to Mn through the *endo* N atoms, namely, N2 (see Table 2 for the atom labeling). This is in contrast to the $[Mn^{III}TtBuPP]^+$ salt, in which the Mn atoms are bonded to the N3 interior nitrogen atoms (Figure 4). The bonding of Mn to N3 requires that the intrachain Mn···Mn separation is shorter than for Mn bonding to N2. This is indeed observed, as the Mn···Mn separation in $[Mn^{III}TtBuPP]^+$ salt is 0.16 Å shorter than in the $[Mn^{III}OEP]^+$ salt. Furthermore, this suggests that the magnetic coupling would be enhanced for the $[Mn^{III}TtBuPP]^+$ salt with respect to the $[Mn^{III}OEP]^+$ salt if the Mn···Mn distance is important. Owing to these anomalies, we thought that the spin distribution on the Mn-bonded N atoms might be sufficiently reduced to lower the intrachain spin coupling. This would be reflected in an attenuated θ value.

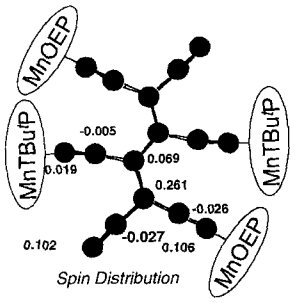

Fig. 4. Illustration of the interior N3 bonding arrangement observed for antiferromagnetically coupled $[Mn^{III}TtBuPP]^+[C_4(CN)_6]^{\bullet -}$ and *endo* N2 bonding arrangement observed for strongly ferromagnetically coupled $[Mn^{III}OEP]^+[C_4(CN)_6]^{\bullet -}$.

As has been reported for $[TCNE]^{\bullet -}$,[16] absolute spin distributions can be directly determined from single-crystal polarized neutron diffraction, and the magnitude of spin distributions can be determined from analysis of the EPR spectra. The EPR-determined spin distribution for $[C_4(CN)_6]^{\bullet -}$ was reported, but it failed to include the spin distribution on C2 and N2 and provided an unreasonably high value of 1.475 μ_B Å^{-3} for N1.[17]

From the detailed study of the spin distribution of $[TCNE]^{\bullet -}$,[16] we have found that density functional theory (DFT) MO calculations provide excellent agreement with experimental observations. Hence, the DFT computation of spin distributions of the isolated $[C_4(CN)_6]^{\bullet -}$ ion was undertaken (Table 4, Figure 4). As observed for $[TCNE]^{\bullet -}$, the sp^2-C and N atoms have positive spin distributions, while the sp-C atoms have negative spin distributions; the magnitudes of the values are comparable. The EPR-derived spin distributions[17] for C1, C3, C4, C5, and N3 are in agreement with the DFT results. However, the value for N1 differs substantially.[18] The key insight from these results is that the N3 spin density (0.019 μ_B Å^{-3}) is more than five times less than that for N2 and N1 (0.104 ± 0.002 μ_B Å^{-3}). This is consistent with a reduced spin coupling between Mn–N3 in $[Mn^{III}TtBuPP]^+[C_4(CN)_6]^{\bullet -}$ with respect to Mn–N2 in $[Mn^{III}OEP]^+[C_4(CN)_6]^{\bullet -}$ and a lower θ value for $[Mn^{III}TtBuPP]^+[C_4(CN)_6]^{\bullet -}$, in accordance with the McConnell model.

The negative effective θ value for $[Mn^{III}TtBuPP]^+[C_4(CN)_6]^{\bullet -}$ is characteristic for antiferromagnetic coupling and is in contrast to the positive value for $[Mn^{III}OEP]^+[C_4(CN)_6]^{\bullet -}$. Since this class of compound exhibits strong intrachain antiferromagnetic coupling, negative θ values are expected from fitting the susceptibility data taken at high temperature to the Curie–Weiss expression. This is observed for $[Mn^{III}TtBuPP]^+[C_4(CN)_6]^{\bullet -}$. For systems with greater antiferromagnetic coupling, such as $[Mn^{III}OEP]^+[C_4(CN)_6]^{\bullet -}$, data taken at higher temperatures are necessary to observe a negative θ. When the antiferromagnetic coupling is sufficiently strong, $\theta < 0$ may not be evident. However, at lower temperatures a linear region in $\chi^{-1}(T)$ is present, which, when fitted to the Curie–Weiss expression, leads to an effective $\theta > 0$ as observed for $[Mn^{III}OEP]^+[C_4(CN)_6]^{\bullet -}$ and $[MnTPP]^+[TCNE]^{\bullet -}$. This signifies net ferromagnetic coupling in this temperature region. A similar region with $\theta > 0$ is not observed for $[Mn^{III}TtBuPP]^+[C_4(CN)_6]^{\bullet -}$ because it is obscured by the rapid decrease in χT below 20 K. We attribute this rapid decrease to the effects of antiferromagnetic interchain interactions suppressing the susceptibility.

Table 4. Comparison of the experimental results with ab initio calculations (basis sets in parentheses). Experimental population values are scaled to yield 1 μ_B per $[TCNE]^{\bullet -}$ and $[C_4(CN)_6]^{\bullet -}$.

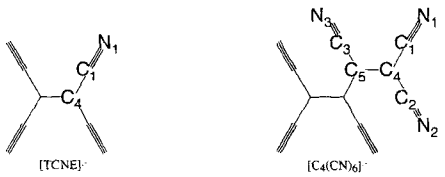

	$[TCNE]^{\bullet -}$			$[C_4(CN)_6]^{\bullet -}$	
	Exp.	NLDFT (TZVP)	DFT (DZVP-LSD)	EPR [17]	DFT (DZVP-LSD)
C1	0.33	0.29	0.28	0.006	−0.026
C2				[a]	−0.027
C3				0.003	−0.005
C4	−0.04	−0.04	−0.04	0.256	0.261
C5				0.080	0.069
N1	0.13	0.15	0.14	1.475	0.102
N2				[a]	0.106
N3				0.023	0.019

[a] Not reported.

Conclusion

Although both $[Mn^{III}TtBuPP]^+[C_4(CN)_6]^{\bullet -}$ and $[Mn^{III}OEP]^+[C_4(CN)_6]^{\bullet -}$ form uniform, linear-chain structures $\cdots D^+A^{\bullet -}D^+A^{\bullet -}\cdots$, the former has the Mn atoms bound to the interior CN nitrogen atoms and exhibits weak antiferromagnetic ($\theta = -13$ K) coupling, while the latter has the Mn bound to *endo* CN nitrogen atoms and exhibits strong ferromagnetic ($\theta = 67$ K) coupling. The weak magnetic coupling is attributed to the interior CN groups having a significantly lower spin density than the outer ones (Figure 4). In addition, the differing orientation of $[C_4(CN)_6]^{\bullet -}$—almost perpendicular for $[Mn^{III}TtBuPP]^+[C_4(CN)_6]^{\bullet -}$ (84.7°) and substantially tilted for $[Mn^{III}OEP]^+[C_4(CN)_6]^{\bullet -}$ (32.1°)—may contribute to poorer overlap and weaker spin coupling, especially with regard to the overlap between the $[C_4(CN)_6]^{\bullet -}$ π^* and the Mn^{III} a_1 SOMO (d_{z^2}) orbitals. However, several related $[TCNE]^{\bullet -}$-containing salts with comparable $[TCNE]^{\bullet -}$–MnN_4 dihedral angles

($>83°$) have double-digit positive effective θ values, and not negative values.[19] This suggests that orientational effects are not as important as the spin distribution for this material. Hence, in addition to a uniform chain structure,[6] binding between sites with large spin densities is needed to stabilize strong ferromagnetic coupling. Further studies are in progress to ascertain the relative importance of orientation and coupling to atoms with large spin densities.

Acknowledgements: The authors gratefully acknowledge support from the US Department of Energy, Division of Materials Science (grant nos. DE-FG02-86ER45271. A000 and DE-FG03-93ER45504) and the National Science Foundation (grant no. CHE9320478). We thank Sandra E. Kalm for discussions and modeling of the magnetic data. K-i. S also acknowledges support by the Monbu-sho (Ministry of Education, Science, and Culture, Japan) fellowship program.

Received: February 8, 1996 [F307]
Revised version: September 16, 1996

[1] a) Proceedings on the Conference on *Ferromagnetic and High Spin Molecular Based Materials* (Eds: J. S. Miller, D. A. Dougherty), *Mol. Cryst. Liq. Cryst.* **1989**, *176*. b) Proceedings on the Conference on *Molecular Magnetic Materials* (Eds: O. Kahn, D. Gatteschi, J. S. Miller, F. Palacio). c) *NATO ARW Molecular Magnetic Materials*, **1991**, *E198*. d) Proceedings on the Conference on the *Chemistry and Physics of Molecular Based Magnetic Materials* (Eds: H. Iwamura, J. S. Miller), *Mol. Cryst. Liq. Cryst.* **1993**, *232/233*. e) Proceedings on the Conference on *Molecule-based Magnets* (Eds: J. S. Miller, A. J. Epstein), *Mol. Cryst. Liq. Cryst.* **1995**, *271–274*.

[2] Reviews: a) A. L. Buchachenko, *Russ. Chem. Rev.* **1990**, *59*, 307; *Usp. Khim.* **1990**, *59*, 529. b) O. Kahn, *Structure and Bonding*, **1987**, *68*, 89. c) A. Caneschi, D. Gatteschi, R. Sessoli, P. Rey, *Acc. Chem. Res.* **1989**, *22*, 392. d) J. S. Miller, A. J. Epstein, W. M. Reiff, *ibid.* **1988**, *21*, 114. e) J. S. Miller, A. J. Epstein, W. M. Reiff, *Science*, **1988**, *240*, 40. f) J. S. Miller, A. J. Epstein, W. M. Reiff, *Chem. Rev.* **1988**, *88*, 201. g) J. S. Miller, A. J. Epstein, *New Aspects of Organic Chemistry* (Eds: Z. Yoshida, T. Shiba, Y. Ohsiro), VCH, New York, **1989**, 237. h) J. S. Miller, A. J. Epstein, *Angew. Chem.* **1994**, *106*, 399; *Angew. Chem. Int. Ed. Engl.* **1994**, *33*, 385. i) J. S. Miller, A. J. Epstein, *Adv. Chem. Ser.* **1995**, *245*, 161. j) D. Gatteschi, *Adv. Mater.* **1994**, *6*, 635. O. Kahn, *Molecular Magnetism*, VCH, Weinheim, 1993.

[3] a) J. S. Miller, J. C. Calabrese, D. A. Dixon, A. J. Epstein, R. W. Bigelow, J. H. Zhang, W. M. Reiff, *J. Am. Chem. Soc.* **1987**, *109*, 769. b) J. S. Miller, J. C. Calabrese, A. J. Epstein, R. W. Bigelow, J. H. Zhang, W. M. Reiff, *J. Chem. Soc. Chem. Commun* **1986**, 1026. c) S. Chittipeddi, K. R. Cromack, J. S. Miller, A. J. Epstein, *Phys. Rev. Lett.* **1987**, *22*, 2695.

[4] J. S. Miller, J. C. Calabrese, R. S. McLean, A. J. Epstein, *Adv. Mater.* **1992**, *4*, 498.

[5] P. Zhou, B. G. Morin, A. J. Epstein, R. S. McLean, J. S. Miller, *J. Appl. Phys.* **1993**, *73*, 6569.

[6] J. S. Miller, C. Vazquez, N. L. Jones, R. S. McLean, A. J. Epstein, *J. Mater. Chem.* **1995**, *5*, 707.

[7] a) B. J. Conklin, S. P. Seller, J. P. Fitzgerald, G. T. Yee, *Adv. Mater.* **1994**, *6*, 836. b) M. Kitano, Y. Ishimari, K. Inoue, N. Koga, H. Iwamura, *Inorg. Chem.* **1994**, *33*, 6012.

[8] a) E. Dormann, *Syn. Met.* **1995**, 71, 1781. b) H. Winter, E. Dormann, R. Gompper, R. Janner, S. Kothrade, B. Wagner, H. Naarmann, *J. Magn. Magn. Mater.* **1995**, *140–144*, 1443. c) H. Winter, M. Klemen, E. Dormann, R. Gompper, R. Janner, S. Kothrade, B. Wagner, *Mol. Cryst. Liq. Cryst.* **1995**, *273*, 111.

[9] A. Böhm, C. Vazquez, R. S. McLean, J. C. Calabrese, S. E. Kalm, J. L. Manson, A. J. Epstein, J. S. Miller, *Inorg. Chem.* **1996**, *36*, 3083.

[10] J. S. Miller, C. Vazquez, J. C. Calabrese, R. S. McLean, A. J. Epstein, *Adv. Mater.* **1994**, *6*, 217.

[11] F. Palacio, J. Ramos, C. Castro, *Mol. Cryst. Liq. Cryst.* **1993**, *232*, 173.

[12] a) H. M. McConnell, *Proc. R. A. Welch Found. Chem. Res.* **1967**, *11*, 144. b) J. S. Miller, A. J. Epstein, *J. Am. Chem. Soc.* **1987**, *109*, 3850.

[13] a) D. D. Perrin, W. L. F. Armarega, *Purification of Laboratory Chemicals 3rd Edition*, Pergamon Press, Oxford, **1988**. b) L. R. Milgrom, *Tetrahedon* **1983**, *39*, 3895. c) T. Ozawa, A. Hanaji, *Inorg. Chim. Acta* **1987**, *130*, 231. d) R. D. Jones, D. A. Summerville, F. Basolo, *J. Am. Chem. Soc.* **1978**, *100*, 4416. e) Y. Naruta, M.-a. Sasayama, T. Sasaki, *Angew Chem.* **1994**, *106*, 1964; *Angew. Chem. Int. Ed. Engl.* **1994**, *33*, 1839.

[14] a) O. W. Webster, *J. Am. Chem. Soc.* **1962**, *84*, 3370. b) D. A. Dixon, J. C. Calabrese, J. S. Miller, *J. Phys. Chem.* **1991**, *95*, 3139. c) J. S. Miller, J. H. Zhang, W. M. Reiff, *J. Am. Chem. Soc.* **1987**, *109*, 4584.

[15] UniChem Chemistry Codes SG-5151 1.0, 1991 (Cray Research).

[16] a) A. Zheludev, A. Grand, E. Ressouche, J. Schweizer, B. Morin, A. J. Epstein, D. A. Dixon, J. S. Miller, *J. Am. Chem. Soc.* **1994**, *116*, 7243. b) A. Zheludev, A. Grand, E. Ressouche, J. Schweizer, B. Morin, A. J. Epstein, D. A. Dixon, J. S. Miller, *Angew. Chem.* **1994**, *106*, 1454; *Angew. Chem. Int. Ed. Engl* **1994**, 33, 1397.

[17] M. L. Kaplan, R. C. Haddon, F. B. Bramwell, F. Wudl, J. H. Marshall, D. O. Cowan, S. Gronowitz, *J. Phys. Chem.* **1980**, *84*, 427.

[18] The value for N in $[TCNE]^{\cdot-}$ [17] is 0.15 μ_B Å^{-3}. Furthermore, assuming that the spin distributions on C1 and N1 are comparable to those on C2 and N2, as has been confirmed by calculation, the results provide a total spin of 6.6 μ_B per unit of $[C_4(CN)_6]^{\cdot-}$. This is over six times the actual value.

[19] E. J. Brandon, J. S. Miller, unpublished results.

[20] Crystallographic data (excluding structure factors) for the structure reported in this paper have been deposited with the Crystallographic Data Centre as supplementary publication no. CCDC-1220-41. Copies of the data can be obtained free of charge on application to The Director, CCDC, 12 Union Road, Cambridge CB21EZ, UK (Fax: Int. code +(1223)336-033; e-mail: teched@chemcrys.cam.ac.uk.